Available online at www.sciencedirect.com
ScienceDirect
Journal of Magnetic Resonance 192 (2008) 27–36
JMR Journal of Magnetic Resonance
www.elsevier.com/locate/jmr

Probing restrictive diffusion dynamics at short time scales

Andrew J.M. Kiruluta

Department of Physics, Harvard University, Jefferson Physical Laboratories, 17 Oxford Street, Cambridge, MA 02138, USA

Received 25 October 2007; revised 13 January 2008
Available online 5 February 2008

Abstract

Diffusion imaging gradients serve to spectrally filter the temporally evolving diffusion tensor. In this framework, the design of diffusion sensitizing gradients is reduced to the problem of adequately sampling q-space in the spectral domain. The practical limitations imposed by the requirement for delta-function type diffusion-sensitizing gradients to adequately sample q-space, can be relaxed if these impulse gradients are replaced with chirped oscillatory gradients. It is well known that in many systems of interest, dispersion of velocity will itself produce a peak in the velocity correlation function near $w = 0$, while restricted diffusion will manifest itself in the dispersion spectrum at higher frequencies. In this paper, chirped diffusion-sensitizing gradients are proposed and analytically shown to yield an efficient sampling of q-space in a manner that asymptotically approaches that using delta-function diffusion-sensitizing gradient. The challenge is the consequent reduction in diffusion sensitivity as one probes higher frequency dynamics. This problem is addressed by restricting the gradient power to a spectral bandwidth corresponding to the diffusion spectral range of the underlying restrictive geometry. Simultaneous imaging of diffusion and flow at microscopic resolution and at temporally resolvable diffusion time scales thus becomes possible in vivo. Simulations and experiments validate the proposed approach.

Keywords: q-Space; Diffusion tensor; Tractography; NMR microscopy

1. Introduction

In a classic pulse gradient spin–echo (PGSE) experiment originally proposed for the measurement of self-diffusion [1], the resulting echo amplitude and phase depend on the nuclear spin velocity correlation function known as the self-diffusion tensor $D(w)$. The signal in an NMR diffusion experiment can thus be expressed in terms of the spectral diffusion tensor $D(w)$ and the spectral density $S(w)$ of the diffusion-sensitizing gradient as [2]:

$$E_{\Delta}(t) = E(0)\exp\left(\frac{1}{2\pi}\gamma^2\int_{-\infty}^{\infty} D(w)S(w,t)\mathrm{d}w\right) = E(0)\mathrm{e}^{\alpha(t)} \tag{1}$$

with the spectral diffusion tensor $D(w)$, defined as the Fourier transform of the velocity autocorrelation function [8],

$$D_{i,j}(w) = \frac{1}{\pi}\int_0^{\infty} \exp(\mathrm{i}wt') < v_i(t')v_j(0) > \mathrm{d}t' \tag{2}$$

where i and j may take on each of the Cartesian directions x, y and z resulting in a symmetric 3×3 tensor and, the power spectral density of the diffusion gradient $S(w, t)$ is given by:

$$S(w,t) = \frac{1}{w^2}\left|\int_0^{\infty} \exp(-\mathrm{i}wt)\gamma g^*(t')\mathrm{d}t'\right|^2 = \frac{|g(w,t)|^2}{w^2} \tag{3}$$

Now, the full 3 dB spectral range (w_{dB}) of diffusion spectrum $D(w)$ is proportional to the mean free diffusion step time τ_C such that $w_{\mathrm{dB}} = 2\pi/\tau_c^{-1}$ and $v_i(0)v_j(t) = v_j^2 \exp(-t/\tau_c)$. The above analysis shows that the design of a diffusion encoding gradient is similar to that of designing a filter. The encoding gradient $g(t)$ effectively filters the diffusion dynamics more on this later.

With the assumption of a narrow gradient limit such that $\delta \ll \Delta$ while keeping the product $g\delta$ finite, the attenuation of the spin–echo has an explicit relationship to the

E-mail address: kiruluta@physics.harvard.edu

1090-7807/$ - see front matter © 2008 Elsevier Inc. All rights reserved.
doi:10.1016/j.jmr.2008.01.013

spectral density $D_{ij}(w)$ of the translational motion. This narrow gradient approximation is helpful since it allows one to use the propagator formalism to describe the result of the PGSE experiment for restrictive diffusion. In this narrow gradient formulation, the echo attenuation function is inverted to yield an image of the average propagator.

Using the conditional probability $P_s(r|r', \Delta)$ that a molecule starting at position r will move to position r' over a time interval Δ, we may write the echo attenuation as [7]:

$$E(q, \Delta) = \rho(r)P(r|r', \Delta)\exp[i2\pi q \cdot (r' - r)]\mathrm{d}r\,\mathrm{d}r' \quad (4)$$

where $\rho(r)$ is the spin density, q is the reciprocal wave vector $(2\pi)^{-1}\gamma g\delta$ and $P(r, \Delta)$ is the probability that a molecule at any starting position is displaced by $R = r' - r$ over time interval Δ. Hence in the narrow gradient limit, there exist a Fourier transform relationship between the amplitude of the echo and the average propagator describing the spectrum of random displacements.

This relationship exists as long as the q-wave vector is not a function of the spin displacement vector $\vec{R}$. In the very short pulse regime ($\delta \to 0$), this condition is easily satisfied. However, in practice, δ is fairly large relative to Δ and under such conditions, q is a spatial–temporal wave vector (i.e. $q = q(\vec{R}, t)$) and hence the Fourier transform relationship between the echo signal and the diffusion propagator $P_s(\vec{R}, \Delta)$ does not hold [2]. In this case, the spectrum of displacements are not resolvable since the wave vector is spatially varying and hence the propagator $\overline{P}_s(\vec{R}, \Delta)$ becomes weighted by a kernel with a quadratic phase factor in $\vec{R}$. To increase the level of diffusion weighting, and hence the size of imposed phase in q-space, we can increase the pulse width to δ' as in Fig. 1. In this case, the region of equal diffusion weighting that maximizes the resolvability of the higher displacement time regimes is proportionally reduced to $\Delta' - \delta' \ll \Delta - \delta$. For a pulse of duration δ, this steady-state condition persists for a duration $\Delta - \delta$ in which random displacements in this interval are weighted equally such that the detected signal is attenuated in direct proportion to the displacement distance $\vec{R}$. However, all displacements that take place before this steady-state condition is reached are weighted in

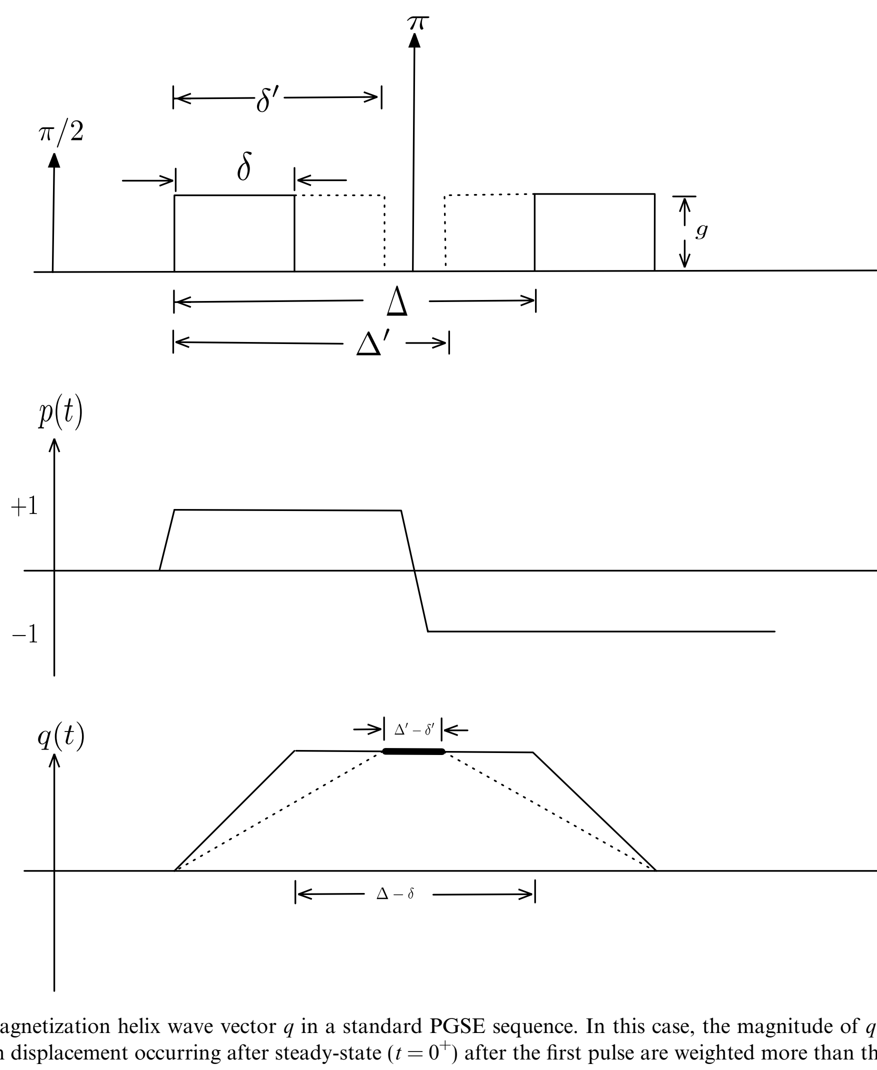

Fig. 1. Evolution of the magnetization helix wave vector q in a standard PGSE sequence. In this case, the magnitude of q is non-zero in the interval Δ indicating that the diffusion displacement occurring after steady-state ($t = 0^+$) after the first pulse are weighted more than those close to the 180° pulse as the q-wave vector increases linearly towards its steady-state value.

proportional to the gradient strength and hence the ability to uniquely resolve spin displacements is completely lost. In addition, according to Eq. (3), the spectrum of resolvable diffusion dynamics is low pass filtered to that of slow diffusion dynamics. It is clear from Fig. 1 that in order to increase the level of diffusion weighting while at the same time ensuring that the wave vector q is the same across the entire displacement spectrum, we require that $g \to \infty$ while $\delta \to 0$. This also allows the spectral sampling of the entire diffusion spectrum. This is indeed the q-space approach first proposed by Callaghan et al. [7]. In what follows, we show that these impulse gradients can be replaced with chirped gradients which are shown to approximate the short pulse field gradient requirement when integrated over a few cycles of the chirp waveforms as long as the chirp bandwidth spans the underlying frequency spectrum of the diffusion dynamics.

Let us start with a standard oscillating gradient spin–echo (OSGE) diffusion sequence first proposed by Gross and Kosfeld [3] and shown in Fig. 2, with the duration of each gradient δ, chosen to be an integral number n of cycles of the oscillations in the restrictive media.

Each cycle of the oscillating gradients acts as a bipolar pulse so that there is a positive gradient lobe followed by a negative gradient lobe of equal area. After each cycle, stationary spins have their magnetic moment rephased whereas diffusing spins lose coherence. The degree of dephasing of the net transverse magnetization is proportional to the mean square displacement of the spins during the effective diffusion time Δ_{eff} which for OSGE sequence is $\frac{3}{8}T$, where T is the period of oscillation [3].

The diffusion coefficient is probed in the form $D(T)$, where T is the period of gradient oscillation. By probing over a range of $D(T)$ spanning a spectrum of gradient oscillating intervals T, the behavior of diffusing spins from short to long periods can be used an indicator of tortuosity changes and compartmentalization [5,6].

Note that in the conventional PGSE, the echo time Δ and the effective diffusion time t are mutually dependent ($t = \Delta - \frac{\delta}{3}$, where δ is the duration of the rectangular PGSE gradient pulses). However, in OGSE, the diffusion-sensitive magnetization helix is present only during the application of the two gradient pulses (δ), but not during the time interval

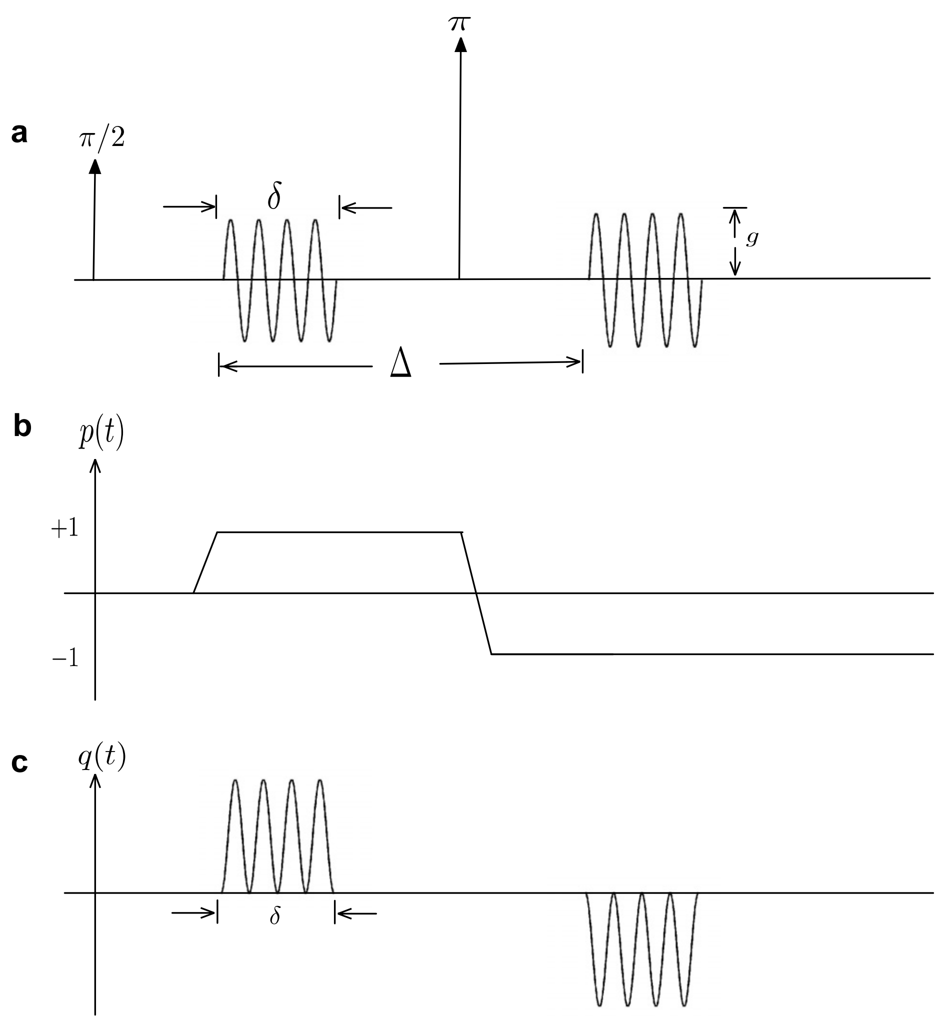

Fig. 2. Oscillating gradient spin–echo sequence for diffusion probing.

between them ($\Delta - \delta$) as in the case of PGSE. Therefore, unlike in the PGSE diffusion experiments, molecular displacements in OGSE are measured on time scale of its duration δ rather than the time separation between the gradient pulses. This enables the measurement of the diffusion at shorter time scales than those accessible in PGSE measurements. The accessibility of short time diffusion makes OGSE an attractive option for studies of restricted diffusion, packed bead flow, or intermediate chemical exchange as well as velocity autocorrelation function in the presence of slow motion or restricted diffusion [4].

Now consider the case of q-space imaging where the PGSE sequence consists of idealized delta functions as shown in Fig. 3. The first delta function produces an almost instantaneous phase shift, depending on the position of each spin in the direction of the field gradient at that time. Stationary spins have their phase unwound by the second delta-function gradient whereas migrating spins have their random displacements encoded in the residual phase of the echo. The instant nature of the diffusion gradient ensures that all spins are encoded at the same time and uniformly.

It is instructive to look at the temporal evolution of the diffusion-sensitizing magnetization helix represented by the q-wave vector as before but with $g(t) = \delta(t)$:

$$q(t) = \int_0^t \gamma p(t')g(t')\mathrm{d}t' = \gamma \int_0^t p(t')\delta(t')\mathrm{d}t = \begin{cases} \gamma p(0) & \text{for } t_1 < t \leqslant t_2, \\ 0 & \text{elsewhere.} \end{cases} \tag{5}$$

In this case, only diffusion changes in position occurring between the two gradient pulses are important and are equally weighted regardless of when they occur within the Δ time interval. By contrast, whereas in the conventional PGSE, a change in position affects the echo amplitude more when it occurs near the 180° pulse than if it occurs near the 90° pulse or just before the echo, in the idealized delta gradient pulse case, all random displacements within the observation interval Δ are equally weighted by the impulse gradient pulse at the beginning of the interval. Since the ensemble of diffusion displacements are equally weighted during the observation interval Δ, the propagator can thus be recovered by inversion of Eq. (4). We can also visualize a scenario where we employ a crafted gradient waveform that

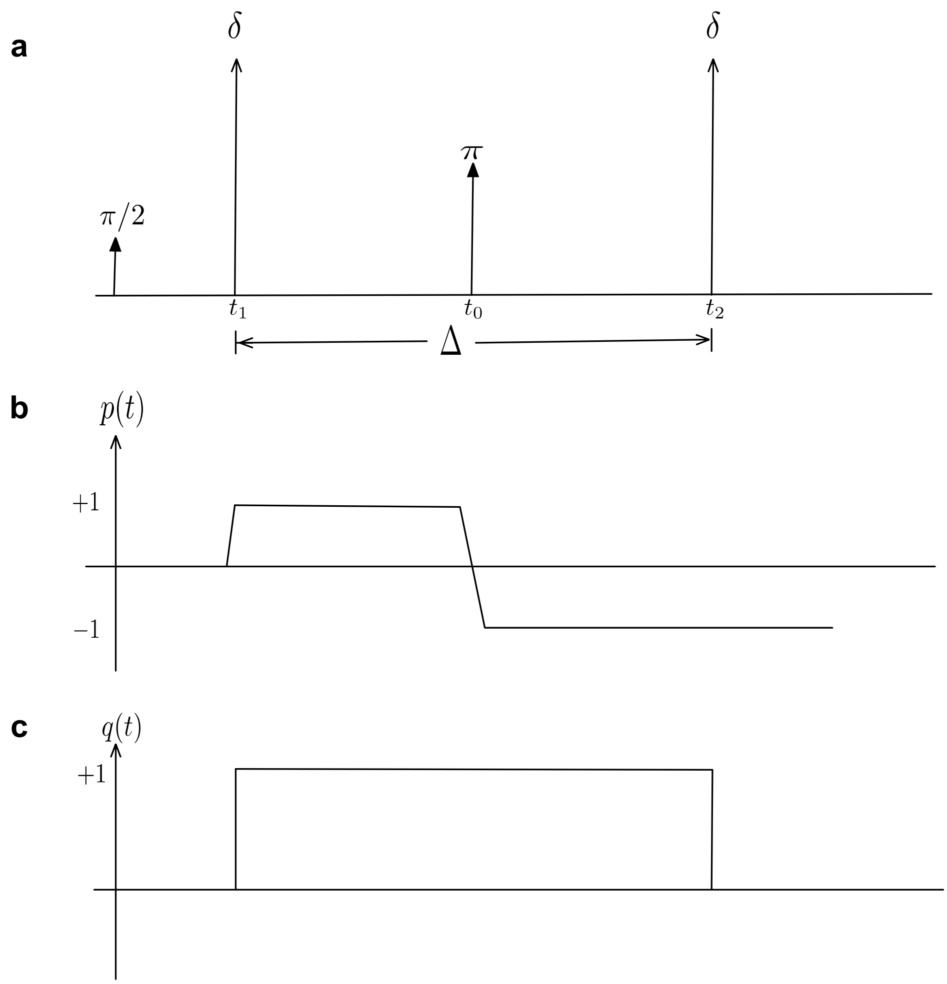

Fig. 3. Evolution of the magnetization wave vector q in the case of delta-function diffusion gradient showing a uniform weighting of spins during the entire diffusion-weighting duration Δ.

discretely samples $q(t)$. Ideally we would sample the diffusion displacements during the observation time with a comb of delta-function weighting pulses. In practice, a version of a sinc sampling function would approximate this weighting in the integration kernel-more on this later.

Let us return to the use of oscillating gradients as diffusion sensitizing gradients. Consider a simple sine wave of frequency f_1. Its q wave vector is a sampling kernel in q-space which asymptotically approaches a delta function for $\delta \to 0$ as the number of cycles $N \to \infty$. During the diffusion probing oscillatory pulse period, only displacements on the order of the frequency of the pulse will be recorded. If the diffusion time is too short, then the displacements will exceed the coherence observation time of the probing gradient period and the overall impacted phase on such displacements will be zero. From the evolution of the q wave vector we can surmise that the random displacement's inverse of the step time (τ_c^{-1}) must be within the bandwidth of the diffusion-sensitizing gradient pulse bandwidth. Higher frequencies of the pulse correspond to probing fast diffusion time regimes while correspondingly lower frequencies probe the slow diffusion regime. We can thus tailor the diffusion gradient to a range of time scales allowing the inverse imaging of the underlying restricting geometry [4].

A discretization version of this approach that allows probing of a range of diffusion time scales leads us to the chirp diffusion weighted gradient approximation developed here. This sampling ensures that a whole spectrum of displacements within the observation time Δ are equally weighted by the phase of the sensitizing pulses.

To fully appreciate the role of the chirp in sampling q-space, consider its coverage of q-space. As in the OSGE case, the period of each resolvable gradient oscillation frequency governs the effective diffusion time regime probed. As the gradient oscillation frequency decreases, the effective diffusion probing time Δ_{eff} increases corresponding to the tracking of long diffusion time species. Conversely, at higher gradient chirp frequencies, the effective diffusion time decreases allowing the probing of the short time diffusing spins. We can thus discretely probe the entire spectrum of diffusion regimes using such chirped gradient waveforms. We generalize here to the case of chirped diffusion gradient waveforms (Fig. 4) which registers diffusion spins from the slow to the fast time regimes as the chirp sweeps over its frequency range. The wave vector q of the diffusion-sensitizing magnetization helix in this case is thus given by:

$$q(t) = g \int_0^t \gamma p(t') \mathrm{e}^{-\mathrm{i}2\pi\kappa t'^2} \mathrm{d}t' \tag{6}$$

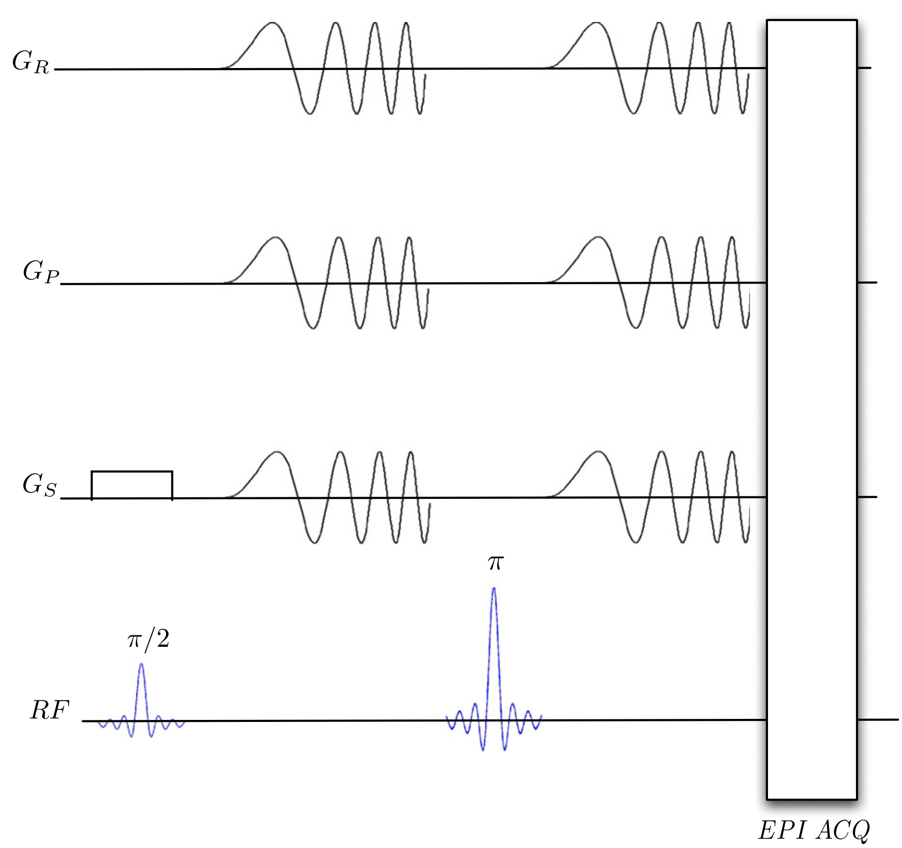

Fig. 4. Timing diagram of proposed diffusion-sensitizing sequence showing the chirp gradient waveforms that are designed to encode the diffusion spectrum.

a solution of which is derived in the next section. We show analytically that in this formulation, the q-space interpretation of the diffusion propagator approach falls out naturally in the high chirp rate limit. This chirped gradient form has a Fourier transform relationship to the diffusion propagator similar to that of the delta-function formulation.

The extent of diffusion spectral sampling of the various encoding gradients (PGSE, OGSE and q-space) in comparison to the chirped gradient scheme proposed here is shown in Fig. 5. In a spin–echo diffusion gradient experiment, sensitization to diffusion arises from sampling the spectral density of the motion with a function $S(w,t)$, which is characteristic of the gradient encoding spectrum. In the idealized case with two delta-function gradient encoding, the sampling is over all possible diffusion rates in the sample, Fig. 5d. The proposed chirped gradient encoding generates discretized approximations to this condition as determined by the chirp extent and is shown in Fig. 5c.

The high frequency diffusion sampling peaks in the spectrum of the diffusion-sensitizing gradients become narrower as the number of oscillation cycles, n, increases and as $n \to \infty$, the expression for $S(w,t)$ reduces to a linear combination of delta functions. For a chirped diffusion gradients, we have that for large n, and for an evolution period t,

$$S(w,t) \to 2\pi g^2 \sum_{m=0}^{N} \frac{1}{w_m^2} t\delta(w \pm w_m) \tag{7}$$

and the attenuation exponent in the diffusion equation can be thus written as:

$$\alpha(t) = \gamma^2 g^2 \sum_{i=0}^{N} \frac{1}{2w_i^2} tD(w_i) \tag{8}$$

which is essentially the product of $D(w)$ with the power spectrum density of the applied gradient. This spectral range should ideally coincide with the spectral range of the diffusion dynamics of the full diffusion tensor matrix.

Note that α depends on the product $(g/w_i)^2 t$. Unfortunately, for chirp diffusion gradient encoding, on increasing the modulation frequency in order to scan higher frequencies, it is necessary to similarly increase the gradient amplitude g in order to maintain the attenuation of the echo. Hence, a chirped gradient encoding scheme will show more sensitivity to low frequency diffusion dynamics.

To compensate for this loss in effective gradient strength due to chirping, the gradient amplitude is linearly increased

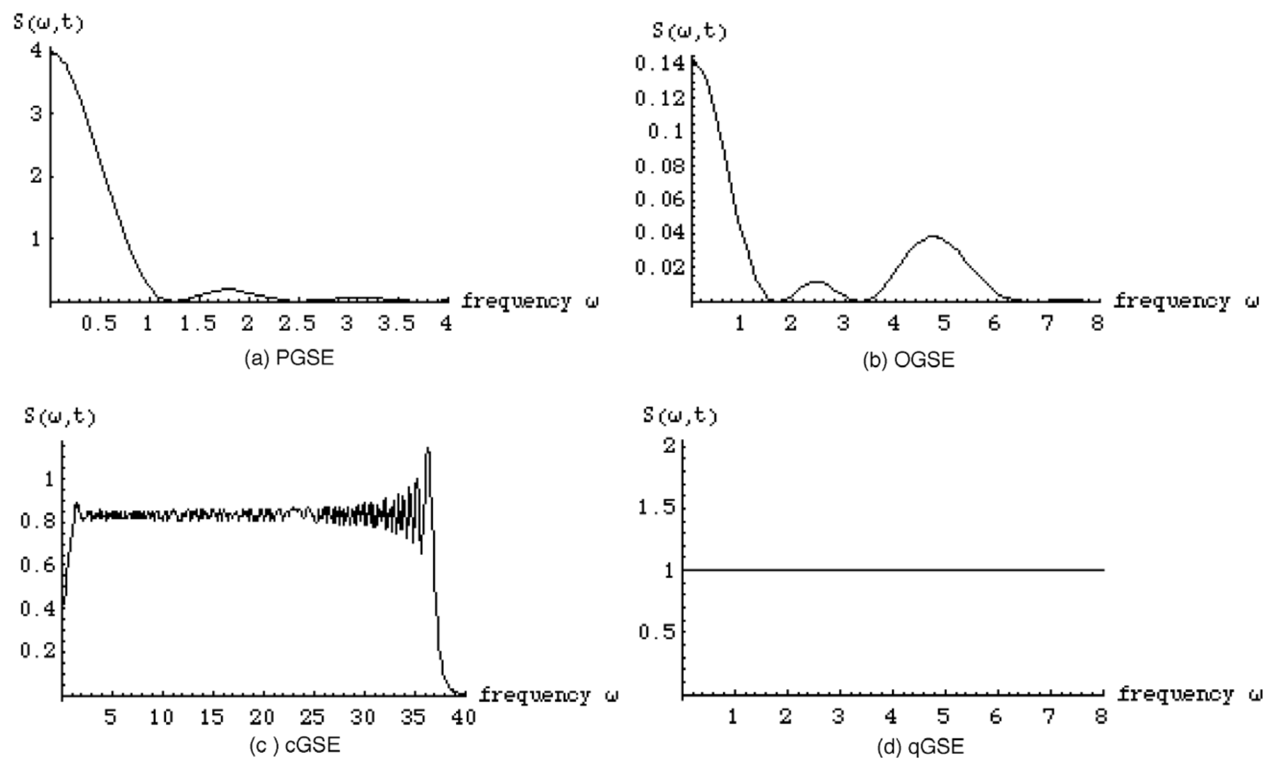

Fig. 5. Spectrum of the diffusion-sensitizing gradient showing range of diffusion spectrum sampling in case of: (a) pulsed gradient experiment (b), oscillating gradient encoding pulse (OGSE) (c), chirped gradient pulse (c) and idealized delta encoding approach corresponding to the interrogation of all possible diffusion time scales. (d) The spectral response shows the range diffusion time scales probed by the various sensitizing techniques. Ideally, the delta-function gradient encoding (d) probes all time scales while the conventional PGSE approach (a) is dominated by low to DC diffusion temporal changes and OGSE (b) probes diffusion time constants that are resonant with the oscillating gradient frequency. By sweeping over a range of frequencies, the chirp gradient approach (c) can be made to asymptotically approach the case in (d) but at the expense of diffusion encoding sensitivity. This issue is resolved by using a coincident RF pulse to amplify the diffusion phase encoding.

with frequency in a modified approach herein referred to as the modified chirped gradient spin–echo (MCGSE). This idea further developed in the next section.

1.1. Modified chirped gradient spin–echo (MCGSE)

On increasing the diffusion gradient modulation frequency in order to scan higher frequencies, it is necessary to similarly increase the gradient amplitude g if the attenuation of the echo over the diffusion bandwidth $D(w)$, is to be retained. To address this problem, a modified chirped gradient spin–echo (MCGSE) is proposed such that:

$$G(t) = g\frac{(w_o + 2\pi\kappa t)}{w_1}\cos(w_o t + \pi\kappa t^2) \tag{9}$$

so that the chirp rate given by:

$$\kappa = \frac{w_1 - w_o}{2\pi\sigma}$$

where w_1 and w_o are the maximum and minimum frequencies, respectively, of the chirped gradient. The gradient wave vector $q(t)$ is then given by:

$$q(t') = \frac{\gamma}{2\pi}\int_0^{t'} G(t)\mathrm{d}t = \frac{\gamma g}{w_1}\sin(w_o t' + \pi\kappa t'^2) \tag{10}$$

so that the b-value is then given by:

$$b = \int_0^{t_s} q^2(t')\mathrm{d}t' = \left(\frac{\gamma g}{w_1}\right)^2 (II_1 + II_2 + II_3) \tag{11}$$

where

$$II_1 = \sigma - \frac{1}{\sqrt{4\kappa}}[\cos(E)[C(F) - C(G)] + \sin(E)[S(F) - S(G)]]$$

$$II_2 = \Delta\sin^2(A)$$

and

$$II_3 = -2\sin(A)\frac{1}{\sqrt{2\kappa}}[\cos(B)[S(c) - S(D)] - \sin(B)[C(c) - C(D)]]$$

with the parameters: $A = w_o\sigma + \pi\kappa\sigma^2$, $B = \frac{w_o^2}{4\pi\kappa}$, $c = \frac{w_o + 2\pi\kappa\sigma}{\sqrt{2\pi^2\kappa}}$, $D = \frac{w_o}{\sqrt{2\pi^2\kappa}}$, $E = \frac{w_o^2}{2\pi\kappa}$, $F = \frac{2w_o + 4\pi\kappa\sigma}{\sqrt{4\pi^2\kappa}}$ and $G = \frac{2w_o}{\sqrt{4\pi^2\kappa}}$. with $C(\cdot)$ and $S(\cdot)$ as two Fresnel integrals defined, respectively, as $C(x) = \int_0^x \cos(t^2)\mathrm{d}t$ and $S(x) = \int_0^x \sin(t^2)\mathrm{d}t$.

For the case when $w_1 = w_o$ or $\kappa = 0$, we have:

$$\lim_{\kappa\to 0} b = \frac{N}{4}\left(\frac{\gamma g}{w_o}\right)^2 \tau^3 \tag{12}$$

where $\sigma = N\tau$, which agrees with the expected b-value formula for an OGSE of cosine modulation.

1.2. Diffusion spectra of MCGSE

The echo amplitude following a diffusion-weighting gradient has a spectral interpretation [9,10] such that the gradient modulation spectrum $F(w)$ of $g(t)$ is given by:

$$\begin{aligned} F(w) &= \int_{-\infty}^{\infty} \mathrm{d}t' \exp(\mathrm{i}wt') \int_0^{t'} \mathrm{d}t''\gamma\mathbf{g}'' \\ &= \int_{-\infty}^{\infty} \mathrm{d}t' \exp(\mathrm{i}wt') q(t') \end{aligned} \tag{13}$$

In practice, $F(w)$ is a vector, since the gradient is generally modulated along one axis. As in conventional experiments, we measure $D(w)$, the diffusion tensor projected onto a unit vector in the direction of the diffusion gradient pulse.

The wave vector $q(t')$ in Eq. (10) can be written as:

$$\begin{aligned} q(t') &= \frac{\gamma g}{w_1 2\mathrm{i}}\exp[2\pi\mathrm{i}(\kappa t'^2/2 + w_o t'/2\pi)] - \frac{\gamma g}{w_1 2i} \\ &\quad \times \exp[2\pi\mathrm{i}(-\kappa t'^2/2 - w_o t'/2\pi)] \\ &= q_1(t') + q_2(t') \end{aligned} \tag{14}$$

Substituting the wave vector into Eq. (13) gives:

$$F(w) = F_1(w) + F_2(w) \tag{15}$$

where $F_1(w)$ and $F_2(w)$ are the Fourier transform of $q_1(t')$ and $q_2(t')$, respectively.

Since diffusion weighting depends on $|F(w)|^2$, the resulting diffusion-weighted echo measurement can be given in terms of the diffusion spectrum, $D(w)$, as in Eq. (1) such that $S(w) = \frac{1}{w^2}|F(w)|^2$. Multiplying $F(w)$ in Eq. (15) by it's conjugate, we get:

$$\begin{aligned} |F(w)|^2 &= |F_1(w)|^2 + |F_2(w)|^2 + F_1^*(w)F_2(w) \\ &\quad + F_2^*(w)F_1(w) \end{aligned} \tag{16}$$

The cross terms in Eq. (16) were checked numerically and found to be dominated by the first two power terms. To further simplify, we will use the relationship between fractional Fourier transforms and Wigner distributions, where the Wigner distribution of a function $f(t)$ defined as [15]:

$$W[t, v] = \int f(t + t'/2)f^*(t - t'/2)\exp(-2\pi\mathrm{i}vt')\mathrm{d}t' \tag{17}$$

with $v = w/2\pi$.

Using one of the properties of Wigner distributions:

$$|F(v)|^2 = \int W(t, v)\mathrm{d}t \tag{18}$$

Eq. (16) can then be expressed as:

$$|F(v)|^2 \simeq \int W_1(t, v) + \int W_2(t, v) \tag{19}$$

Recalling the Wigner distribution of some elementary functions, $f(t) = \exp[2\pi\mathrm{i}(b_2 t^2/2 + b_1 t + b_o)] \Rightarrow W(t, v) = \delta(b_2 t + b_1 - v)$ the spectra in Eq. (16) can be written as:

$$\begin{aligned} |F(w)|^2 &\simeq \left(\frac{\gamma g}{w_1 2}\right)^2 \left[\int \delta(\kappa t + v_o - v)\mathrm{d}t + \int \delta(-\kappa t - v_o - v)\mathrm{d}t\right] \\ &\simeq 2\left(\frac{\gamma g}{w_1 2}\right)^2 \int_0^\sigma \delta\left(\left(\frac{v_1 - v_o}{\sigma}\right)t + v_o - v\right)\mathrm{d}t \simeq \frac{\gamma^2 g^2}{w_1^2 2}\int_0^\sigma \delta(h(t))\mathrm{d}t \end{aligned} \tag{20}$$

where

$$h(t) = \left(\frac{v_1 - v_o}{\sigma}\right)t + v_o - v$$

Using the scaling property of delta function:

$$\delta(h(t)) = \frac{\delta\left(t - \left(\frac{v - v_o}{v_1 - v_o}\right)\sigma\right)}{\left(\frac{v_1 - v_o}{\sigma}\right)} \quad (21)$$

We find that the integral in Eq. (20) is non-zero only for the condition:

$$t = \left(\frac{v_1 - v_o}{v_1 - v_o}\right)\sigma = \left(\frac{w_1 - w_o}{w_1 - w_o}\right)\sigma$$

or

$$w = \frac{t}{\sigma}(w_1 - w_o) + w_o$$

in the range:

$0 < t \leqslant \sigma$

the former condition is fulfilled only for the frequency bandwidth:

$w_o \leqslant w \leqslant w_1$

where w_o and w_1 are the initial and the final frequencies, respectively, in the MCGSE and,

$$|F(w)|^2 = \frac{\gamma^2 g^2}{2w_1^2}\int_0^\sigma \delta(h(t))\mathrm{d}t = \begin{cases} \text{constant} & \text{for } w_o \leqslant w \leqslant w_1, \\ 0 & \text{elsewhere.} \end{cases} \quad (22)$$

Fig. 5 shows the spectral diffusion sampling functions for various sensitizing gradient types. The comparison of the power spectral $|F(w)|^2$ in (c) and (a) for MCGSE and PGSE, respectively, shows the advantage of MCGSE in covering a required diffusion-sensitization frequency bandwidth while the sensitization in PGSE is always centered at DC and hence insensitive to fast diffusion time constants or the investigation of short time scale diffusion, compared to the case depicted in (d) for the ideal δ-gradient where it covers the entire spectrum evenly. We see that even though the δ-gradient evenly probes all diffusion time scales, it is nevertheless wasteful of power since realistic restrictive geometries do not have an infinite bandwidth of diffusion time scales. The MCGSE scheme proposed here addresses this question by only probing the diffusion time scales relevant to a given restrictive geometry under study and hence is more robust to practical implementation. The result is an overall higher power spectral density of the diffusion encoding gradient for each of the frequencies in $D(w)$ of the restrictive media.

2. Analysis and discussion

In restrictive geometries, the Fourier spectrum of the confinement space appears explicitly in the measurement, an effect which has been termed diffusive diffraction. One of the problems with PGSE q-space diffraction experiments is the requirement of the scattering formalism for an approximation of the gradient waveform with two narrow pulses. In particular, it is assumed that not only is the duration δ of the pulses much smaller than their separation Δ, but that the distance diffused during the pulses is small compared with characteristic dimensions of the pore space morphology. A number of authors have recently addressed the issue of q-space diffraction under conditions of finite gradient pulse widths, both in qualitative terms [12] and by simulations [11,16]. A significant and successful analytical treatment of the finite pulse problem was demonstrated by Caprihan et al. [13] using the approach of multiple propagators. This approach was much simplified by Callaghan [14] with the echo signal $E_q(\Delta)$ being expressed as a product of matrix operators. We use this approach in calculating $E_q(\Delta)$ for a chirped gradient waveform. This chirped waveform can be expressed in terms of the multiple propagators using a descritized envelope function expressed by N impulses of integer multiple g_m at spacing τ such that $\Delta = (N + 1/2)\tau$ and $\sigma = (M + 1/2)\tau$.

Hence:

$$E_q(\Delta) = S(q)\left[\prod_{n=1}^{M} RA(q)^{g_m}\right]R^{N-M}\left[\prod_{n=1}^{M} RA^\dagger(q)^{g_m}\right]RS^\dagger(q) \quad (23)$$

where $g_m = \text{round}(G_m\cos(\pi\kappa(m\tau)^2))$ with $G_m = \text{round}(g_{\max}/g_{\text{step}})$, and round$(\cdot)$ as the round-down operator.

For the planar boundary case, the eigenfunction solutions in the case of perfectly reflecting walls at $x = 0$, are:

$$P(\mathbf{r}|\mathbf{r}', t) = \sum_{n=0}^{\infty} \exp(-\lambda_n t)u_n(\mathbf{r})u_n^*(\mathbf{r}') \quad (24)$$

where

$$\begin{aligned}
&u_o = (1/a)^{1/2} \\
&u_n = (2/a)^{1/2}\cos(\kappa\pi x/a) \\
&S = BS' \\
&A = C^\dagger A' C \\
&R = \exp(-\lambda_n\tau) \\
&\lambda = -n^2\pi^2 D\tau/a^2 \\
&B_{00} = 1/a \\
&B_{nn} = 2^{1/2}/a \\
&C_{00} = (1/a)^{1/2} \\
&C_{nn} = (2/a)^{1/2} \\
&S'_n = \begin{cases} \mathrm{i}2a\exp(\mathrm{i}\pi qa)(2\pi qa)\cos(\pi qa)/((2\pi qa)^2 - (\kappa\pi)^2) & k \neq 0 \text{ odd}, \\ 2a\exp(\mathrm{i}\pi qa)(2\pi qa)\cos(\pi qa)/((2\pi qa)^2 - (\kappa\pi)^2) & k \neq 0 \text{ even} \end{cases}
\end{aligned} \quad (25)$$

and

$$A_{nn'} = \frac{1}{2}[S'_{|n-n'|} + S'_{n+n'}]$$

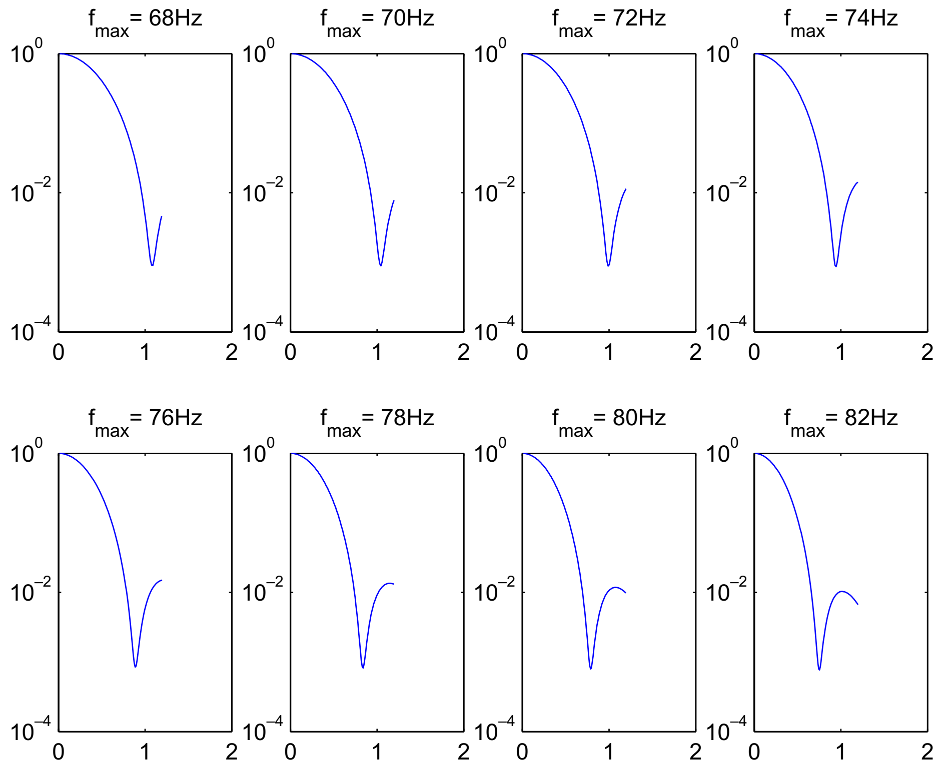

Fig. 6. Shows the oscillating of the first minimum in the diffraction pattern of the signal echo around $qa = 1$ using the chirped waveform gradient at different chirp rate $\kappa = f_{max}/\sigma$ ($f_{max} = 68$–82 Hz), and fixed gradient duration time $\sigma = \Delta/2$. The horizontal axis represents the q-value while the vertical coordinate represents the signal echo amplitude. This result shows that sweeping the gradient frequency achieves the proper pore size parameter at $f_{max} = 72$ Hz as we would expect in the theoretical implementation with a delta-function diffusion-sensitizing gradient. This pore size approximation oscillates from its true value sinusoidally so that within a chirped bandwidth, the true pore size value can be found at one of the frequencies.

where ($'$) and ($\dagger$) indicate matrix transpose and transpose conjugate, respectively.

The diffraction pattern for a chirped waveform with parameters: $\Delta = 0.6a^2/D$, $\sigma = \Delta/2$ and $\kappa = f_{max}/\sigma = 0$ was generated in an experimental setup of a diffusion phantom consisting of two rectangular barriers separated by a distance a. This special case represents the finite gradient pulse case. The experimental results show that (see Fig. 6 at different frequencies), the position of the first minima in $E_q(\Delta)$, using MCGSE, equals qa while for the PGSE approach, it is overestimated to a higher value of qa. This shift increases with the pulse duration or smaller pore size when PGSE is employed. This shrinking in pore size has been discussed by a number of authors [12,16,13]. They concluded that the finite gradient pulse width effectively changes the resultant pore shape, making the isolated pores appear smaller than their actual size. By changing the chirp rate κ, it was found that the position of the first minima oscillates around the value qa as shown in Fig. 6 and at a specific rate, it yields an exact pore size as in the case of q-space imaging with narrow pulse gradients. Hence, chirped diffusion encoding gradients can be used to scan the Fourier space of the diffusive media to yield a minima corresponding to each of the pore geometries in the restrictive media.

3. Conclusion

We have proposed a novel diffusion probing method using chirped gradient waveforms and its usefulness in probing short time diffusion dynamics verified analytically and through simulations. An analytical expression for the b-value of the MGSE approach was derived and shown to collapse to a OGSE experiment when the chirp rate is set zero.

It was shown that using the CGSE diffusion gradients at a specific chirp rate, determined the underlying pore geometry, which makes it a practical alternative to the ideal delta-function pulse gradient. It is the higher frequency lobes in the spectrum of the CGSE that allow sampling of the short time diffusion components. However, these higher frequency lobes are generated at ever decreasing diffusion sensitizing power which reduces the effective bandwidth of the probed diffusion spectrum $D(w)$. This consequent reduction in diffusion probing power inherent in a simple chirped gradient approach is overcome with the proposed MCGSE encoding scheme which is shown to be tunable to any desired diffusion spectral bandwidth.

The chirped gradient approach has the advantage that the available gradient power is restricted to the inherent bandwidth of the diffusion dynamics which increases the

q-value for probing such dynamics. By restricting the spectral bandwidth of the chirp to that of the underlying diffusion dynamics in the restrictive media, the available power is distributed only over that frequency range thus increasing the overall power density. This accomplishes the same q-space sampling of the underlying diffusion as a delta-function gradient in this spectral range but with the practical implementation advantages of using a chirp and without loss of power in probing unnecessary diffusion eigenmodes.

By spreading the available gradient power to the spectral range of diffusion dynamics being probed, MCGSE provides an efficient and practical implementation of q-space techniques on a conventional scanner.

References

[1] E.O. Stejskal, J.E. Tanner, J. Chem. Phys. 42 (1965) 288–292.
[2] P.T. Callaghan, D. MacGowan, K.J. Packer, F.O. Zelaya, J. Magn. Reson. 90 (1990) 177–182.
[3] B. Gross, R. Kosfeld, Messtechnik 77 (1969) 171–177.
[4] P.N. Sen, J. Chem. Phys. 119 (2003).
[5] A.R. Waldeck, P.W. Kuchel, A.J. Lennon, B.E. Chapman, Prog. Nucl. Magn. Reson. Spectrosc. 30 (1997) 39–68.
[6] M. Schachter, M.D. Does, A.W. Anderson, J.C. Gore, J. Magn. Reson. 147 (2000) 232–237.
[7] P.T. Callaghan, C.D. Eccles, Y. Xia, J. Phys. E: Sci. Instrum. 21 (1988) 820–822.
[8] R. Lenk, Brownian Motion and Spin Relaxation, Elsevier, Amsterdam, 1977.
[9] A. Kiruluta, J. Chem. Phys. 124 (2006) 194108.
[10] A. Kiruluta, K. Anderson, G. Barbastathis, J. Opt. Soc. Am. A 23 (6) (2006) 1391–1399.
[11] A. Coy, P.T. Callaghan, J. Chem. Phys. 101 (6) (1994) 4599–4609.
[12] P.P. Mitra, B.I. Halperin, J. Magn. Reson. A 113 (1995) 94–101.
[13] A. Caprihan, L.Z. Wang, E. Fukushima, J. Magn. Reson. A 118 (1996) 94–102.
[14] P.T. Callaghan, J. Magn. Reson. 129 (74) (1997) 84.
[15] H.M. Ozaktas, B. Barshan, D. Mendlovic, L. Onural, J. Opt. Soc. Am. A 11 (1994) 547.
[16] M.H. Blees, J. Magn. Reson. A 109 (1994) 203.